JOURNAL OF Applied Polymer SCIENCE

Special Issue: Sustainable Polymers and Polymer Science Dedicated to the Life and Work of Richard P. Wool

Guest Editors: Dr Joseph F. Stanzione III (Rowan University, U.S.A.)
and Dr John J. La Scala (U.S. Army Research Laboratory, U.S.A.)

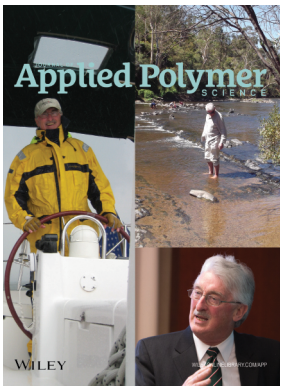

EDITORIAL

REVIEWS

RESEARCH ARTICLES

JOURNAL OF Applied Polymer SCIENCE

Special Issue: Sustainable Polymers and Polymer Science Dedicated to the Life and Work of Richard P. Wool

Guest Editors: Dr Joseph F. Stanzione III (Rowan University, U.S.A.)
and Dr John J. La Scala (U.S. Army Research Laboratory, U.S.A.)

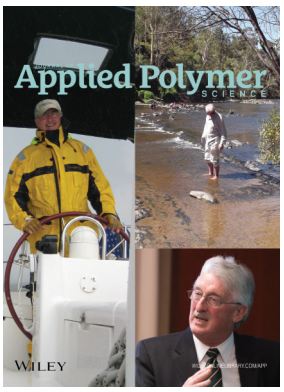

Journal of Applied Polymer Science

Polylactic acid bioconjugated with glutathione: Thermosensitive self-healed networks

Dalila Djidi,[1,2,3] Nathalie Mignard,[1,2,3] Mohamed Taha[1,2,3]
[1]Université De Lyon, Saint-Etienne 42023, France
[2]Ingénierie Des Matériaux Polymères, CNRS, Saint-Etienne 42023, France
[3]Université De Saint-Etienne, Jean Monnet, Saint-Etienne 42023, France
Correspondence to: M. Taha (E-mail: mtaha@univ-st-etienne.fr)

ABSTRACT: Polylactic acid was bioconjugated with glutathione (GSH) in a solvent-free one step process. Thermo-reversible networks were first obtained as a consequence of the supramolecular interactions induced by GSH moieties. Then dynamic covalent reactions were added to the networks' synthesis process using dialcohol-functionalized Diels−Alder (DA) adducts. The main properties of these networks were analyzed in relation with their structures and the proportions of supramolecular and DA reactions. The thermo-mechanical properties of the obtained transparent materials and their healing efficiency were evaluated by dynamic mechanical spectroscopy and tensile analyses. Crosslinking/de-crosslinking temperatures varied from 36 to 112 °C. The obtained networks showed self-healing ability without external stimuli. © 2016 Wiley Periodicals, Inc. J. Appl. Polym. Sci. **2016**, *133*, 43436.

KEYWORDS: biomaterials; glass transition; self-assembly; thermosets

Received 5 October 2015; accepted 13 January 2016
DOI: 10.1002/app.43436

INTRODUCTION

The interest in polymer bioconjugation has been growing widely recently as it is a reliable approach for the creation of new and innovative materials, tuning their properties according to the desired applications. These materials are principally used in the field of synthetic scaffolds, controlled-release, drug carrier systems, and other biomedical fields. They also represent an essential subject in pharmaceutical chemistry.[1–7] Different strategies were used to conjugate polymers to biomolecules.[8,9] These methods are common in the area of macromolecular architecture. They implement (i) bioconjugation by coupling, (ii) direct polymerization from a biomolecule, (iii) inverse bioconjugation approach, (iv) functional monomers and macromonomers and although bioconjugation is by definition a covalent linkage, and (v) noncovalent bioconjugation has been developed during the last few years. Polymer conjugates are built with a wide variety of architectures and macromolecules[3,10–19] like polyethylene glycol for the most encountered of them, N-(2-hydroxypropyl) methacrylate, polyglutamic acid; PLA is also often used in bioconjugation as a copolymer with a hydrophilic polymer.[20–22]

Peptides and proteins represent the most often conjugated biomolecules.[3,15,23] Besides, their bioconjugation may confer to materials specific properties due to the presence of hydrogen bonds in the biological component. it may be advantageous to use hydrogen bonding for the design and preparation of new bioconjugated polymer networks with self-healing ability thanks to crosslinking and decrosslinking properties.

Inspired from biological systems, self-healing materials are able to partially or completely heal/repair/recover damages inflicted on them. This kind of materials receives a particular attention, since they can offer interesting possibilities of applications and expands the lifetime use of the material. They already interest aeronautics,[24,25] and are expected to be used in several domains in the near future.

Mechanical, thermal, electrical, electromagnetic, or release of healing agents were developed as triggers for healing.[26–28] Several dynamic bonds usable for healing polymers have been used.[29–34]

Among them Diels−Alder (DA) [4 + 2] cycloaddition between furan and maleimide[35–48] especially, offers a controllable thermoreversibility that allows repeated reformation and healing ability in response to damage.[49]

Non-covalent interaction were also widely studied property.[34,50–55] A biobased rubber with self-healing ability has been developed by Cordier *et al.* thanks to supramolecular assembly.[34] However, in general, these systems do not show self-healing ability automatically.

In this study, to mimic the natural healing ability in living bodies and to obtain a healing ability without external

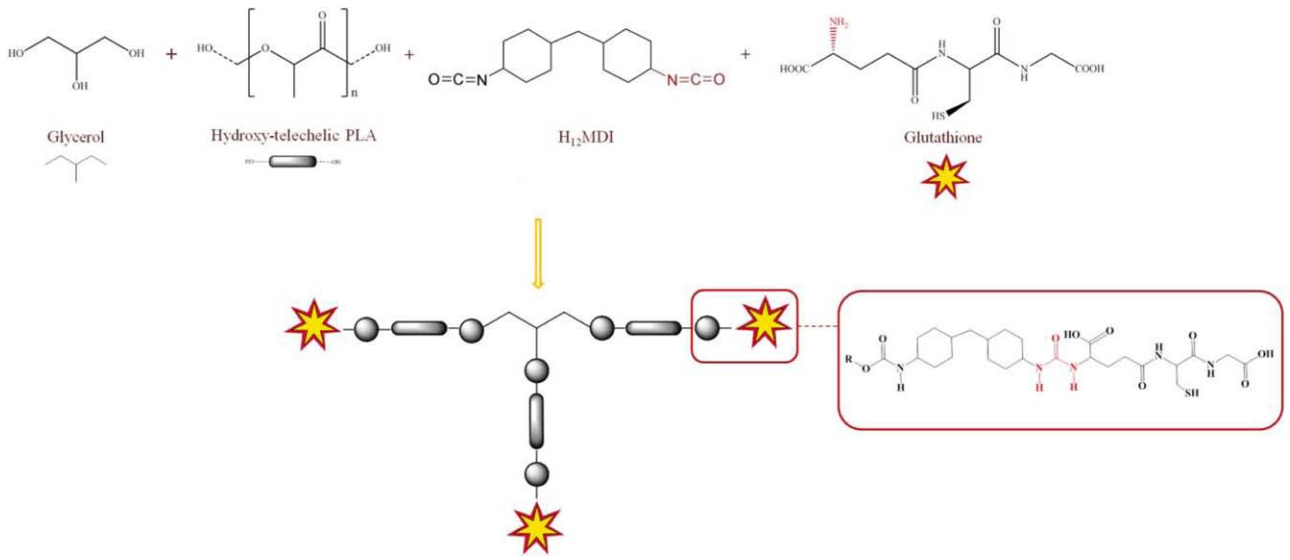

Scheme 1. Schematic and chemical structure representing runs 4 and 6 and the condensation reaction between H_{12}MDI and GSH. [Color figure can be viewed in the online issue, which is available at wileyonlinelibrary.com.]

activation, thermally reversible crosslinked material with a low reversibility temperature is designed. In this aim, Glutathione (GSH) tripeptide was first chemically conjugated to multi-branched −2, 3, and 5 arms- PLA oligomers allowing the formation of supramolecular networks. In a second part, to modulate the properties of the materials, supplementary dynamic links were added- the supramolecular networks were reinforced by a Diels-Alder adduct achieving double dynamic networks. Thermomechanical properties and self-healing ability of reversible networks were studied by evaluating the supramolecular network reinforcement and the structure dimensions effect.

EXPERIMENTAL

Reagents

L-Lactide (from PURAC, PURASORB) with a molecular weight of 144.13 g mol^{-1} was used. 4,4′-Methylene bis(cyclohexyliso-cyanate) (H_{12}MDI, mixture of isomers, 90%), L-GSH reduced (≥98%), maleimide (98%), glycerol (99%), 1,4-butanediol (98%), xylitol (≥99%), formaldehyde (solution 37 wt % in water), catalysts: tin(II)2-ethylhexanoate [Stannous octanoate—Sn(oct)2] (95%), Dibutylin dilaurate (95%), and different solvents: chloroform, dimethylformamide, and ethanol were purchased from SIGMA ALDRICH. The furfuryl alcohol (98%), was purchased from ACROS ORGANICS, and other solvents, tetrahydrofuran, dimethyl sulfoxide (DMSO), petroleum ether and ethyl acetate from CARLO ERBA. Glycerol was dehydrated by 3 Å molecular sieves (rod shape, size 1/16 inch, Fluka) for 48 h. All the other reagents were used as received without further purification.

Bifunctional Diels-Alder Adduct Synthesis

The Diels-Alder adduct was obtained from an equimolar ratio of N-hydroxymethylmaleimide (HMM) and Furfuryl Alcohol (FAl). In a first step, the HMM was synthesized according to Tawney *et al.* protocol.[56] The bifunctional Diels-Alder adduct was then prepared as previously described[57] with a 76% yield and $T_{m\ (DSC)} = T_{rDA} = 141\ °C$.[58]

Synthesis of PLA-Diols

PLA oligomers with different molar masses (3000, 2000, and 800 g mol^{-1}) were synthesized by ring opening polymerization of L-lactide initiated with butanediol -or Diels-Alder adduct for the synthesis of PLA-DA-Diol—as described in a previous work.[26]

Polymer Network Formation

Bi, tri, and penta-functional PLA networks were formed by conjugation of GSH through the condensation reaction between NCO and amine functions (Scheme 1) in DMSO. Multialcohols (glycerol and xylitol), PLA-Diol or PLA-DA-Diol, H_{12}MDI, and catalyst were first dissolved in 10 mL of DMSO in a round-bottomed flask at 80 °C to promote the hydroxyl/isocyanate reaction. After the homogenization of the mixture, the hydroxyl/isocyanate reaction was tracked by FTIR until the isocyanate absorption band at 2200 cm^{-1} was stabilized. Then, the temperature was decreased to room temperature and GSH was added. Tri (Scheme 1) and penta-hybrid networks were synthesized adding dihydroxy-Diels-Alder adduct to the previous reagents. The typical total reaction time was 5 h. The reagents' proportions are given in Table I.

For more details on the protocol, the synthesis of run 4 is given as an example. In a 100 mL round-bottomed dry flask equipped with a nitrogen purge and magnetic stirring, 0.18 g (0.0020 mol) of glycerol, 4.72 g (0.0059 mol) of PLA-Diol (800 g mol^{-1}), 3.15 g (0.0119 mol) of H_{12}MDI, and 0.07 g ($0.0119*10^{-2}$mol) of dibutyltin dilaurate were dissolved in 10 mL of DMSO. The mixture was magnetically stirred at 80 °C until homogenization. Once the mixture homogenized, the temperature was decreased to room temperature and 1.84 g (0.006 mol) of GSH were added to the mixture. The reaction was tracked by FTIR and stopped after the total disappearance of the isocyanate absorption band at 2200 cm^{-1}. The viscous

Table I. Reaction Conditions for the Synthesis of PLA Networks with Different formulations

Runs	Formulation (mol) Multialcohol:PLA: H_{12}MDI:Glu:DA	Multialcohol	PLA arms number	$M_{n\ (PLA)}$ (g mol^{-1})
Run 1	0:1:2:2:0	None	2	800
Run 2	0:1:2:2:0	None	2	2000
Run 3	0:1:2:2:0	None	2	3000
Run 4	1:3:6:3:0	Glycerol	3	800
Run 5	1:5:10:5:0	Xylitol	5	800
Run 6	1:3:6:2:1	Glycerol	3	800
Run 7	1:5:10:2:3	Xylitol	5	800

M_n values were measured by 1H NMR analysis.

product obtained was then dried under vacuum at 40 °C for 72 h. After drying, a transparent product was collected.

Characterizations

- FT-IR absorption spectra were recorded on a Nicolet Nexus spectrometer (500–4000 cm^{-1}) using ATR technique.
- The thermal analyses of PLA-Diol and PLA's networks were performed with a TA Instruments Q10 Differential Scanning Calorimeter DSC. All the samples were analyzed in hermetically sealed pans, in a temperature range of −60–160 °C, with a heating and a cooling rate of 10 °C min^{-1}. Transition temperatures (T_g) were evaluated from the data recorded during heating by identifying the inflection points.
- Molten state rheological analyses were conducted with a stress controlled ANTON PAAR (MCR301) rheometer using 25 mm diameter parallel plate geometry. The gap between plates was around 2 mm. Linear domains were first established for all the samples. The ramp temperature experiments were then performed under dynamic oscillation mode using a 1 rad s^{-1} frequency at a constant ramp temperature of 1 °C min^{-1}. Experiments were performed in heating and cooling cycles, between 30 and 150 °C. The frequency sweep tests were also performed at low and high temperatures at frequency ranges of 10^{-2} and 10^{2} rad s^{-1}.
- Self-healing tests were performed by cutting samples in the middle. The two broken surfaces were then immediately reassembled, subjected to a gentle manual pressure during one minute, and stored at room temperature for 24 h in a controlled atmosphere (25 °C, 60% of humidity) without any continued pressure.
- Tensile analyses were recorded with a Shimadzu Autograph AGS-X series. 1 BB NF EN ISO 527-2 norm dumbbell-shaped specimens were used in tensile testing. The sample's length between two jaws was about 50 mm. For the self-healing efficiency tests, the crosshead speed was controlled at 10mm min^{-1}.

RESULTS AND DISCUSSION

Dynamic and double dynamic bioconjugated networks obtained thanks to supramolecular interactions and the reversible Diels-Alder reaction were prepared and analyzed here. Materials with different structures and concentrations of sticker and/or Diels Alder adduct were synthesized. GSH was conjugated to PLA-based structures using the condensation reaction between residual isocyanate functions of the PLA prepolymers and the GSH amine function. GSH, beside its important antioxidant character, contains several donor and acceptor groups. These donor and acceptor groups participate to the establishment of a supramolecular network. This point will be first developed.

Synthesis and Characterization of Supramolecular Bioconjugated Networks

Bi, tri, and penta- GSH functionalized PLA-based structures were synthesized in this part (run 1–5). Their synthesis is developed in the experimental part; reaction conditions are described in Table I. An example of structure is given in Scheme 1.

The Glutation contains thiol and amine groups. However, even if the thiol is highly reactive with isocyanate, the amine reaction rate with isocyanate is much higher than the reaction rate of thiol with isocyanate.

It was recently clearly demonstrated that in case of a competitive reaction of Thiol and amine with isocyanate, the amine reaction is predominant and no perceptible reaction of thiol with isocyanate was obtained.[59]

Supramolecular interactions provided by the GSH molecules can allow the formation of an assembled polymer network under certain conditions. In general, the presence of crosslinking polymers can be verified by solubility tests. In this work, at room temperature all samples were insoluble in DMSO, a good solvent for all the reactants, indicating the possibility of a presence of networks. It is important to note that these tests are only indicative; other analyses were done to confirm the presence or the absence of networks.

Dynamic Mechanical Spectroscopy in the Molten State

Dynamic mechanical properties of supramolecular bioconjugated network systems are studied in this part. The influence of structure dimensions on reversibility temperatures was evaluated during heating and cooling cycles. Prior to that, frequency sweeps were conducted at low and high temperatures to confirm the crosslinking/decrosslinking behavior of these materials.

At low temperatures [Figure 1(a)], the frequency sweep shows the behavior of a cross-linking material with a G' modulus independent from the frequencies, thus indicating the presence of a network, the G' modulus being always higher than the G'' one. Meanwhile, a liquid-like behavior is observed at higher temperature (100 °C) [Figure 1(b)], indicating the decrosslinking of this system. These analyses confirm the network formation in these systems and demonstrate the thermal-dependence and the reversibility of the supramolecular bioconjugated systems.

In the next part, the thermal-dependence of these systems will be evaluated and the effect of structure dimensions on the reversibility temperatures will be studied.

Dynamic temperature ramps were performed to determine the reversibility temperatures as shown in Figures 2 and 3.

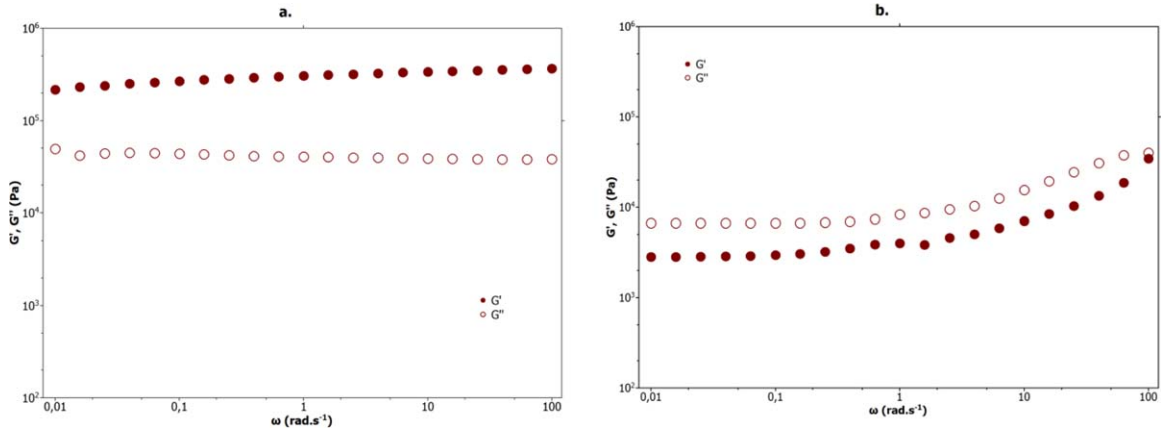

Figure 1. Frequency sweep for supramolecular bioconjugated system (run 4) (**a**) at 30°C and (**b**) at 100°C. [Color figure can be viewed in the online issue, which is available at wileyonlinelibrary.com.]

Dynamic mechanical spectroscopy (runs 1–3) demonstrates that networks were obtained even when bifunctionalized (linear) oligomers were used. To explain this experimental fact, it should be considered that more than two GSH units were gathered together thanks to secondary interactions. These assemblies represent the cross-linking points, connecting more than two chains and leading to three-dimensional assemblies (Scheme 2).

Besides, dynamic mechanical spectroscopy indicated that the main properties of these materials, based on difunctional polymers assemblies (runs 1–3), were influenced by the PLA molar masses (Table II). Figure 2 shows an example (run 2) of the moduli evolution with temperature. The crossover of G' and G'' moduli represents the crosslinking/decrosslinking temperature of the network and is of 80 °C for run 2; this temperature is different for the others networks (runs 1 and 3).

To study the influence of the prepolymers architecture on the thermomechanical properties, two different systems were created using the same PLA as for run 1 (800 g mol^{-1}) with a view to obtaining low reversibility temperatures. Runs 4 and 5 were synthesized using glycerol and xylitol as multialcohol, respectively.

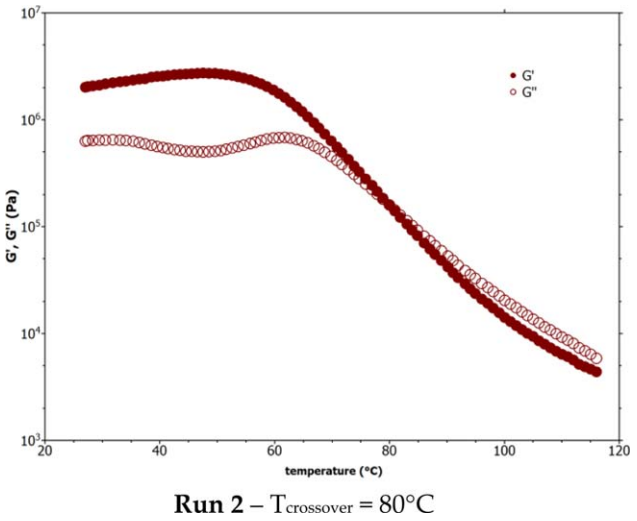

Figure 2. Dynamic temperature sweeps for the supramolecular bioconjugated system (run 2) at 1 rad s^{-1} - first heating cycle. [Color figure can be viewed in the online issue, which is available at wileyonlinelibrary.com.]

Analysis reported in Figures 1(a) and [3] were performed on an equivalent sample(Run 4) at the same temperature "30 °C" and frequency 1 rad s^{-1}; the moduli, and particularly G', are plainly higher in Figure 1(a).

This difference is a consequence of the dynamic character of the assemblies. The experiment reported in Figure 1(a) (frequency sweep) was made after an ageing period. During this period, an equilibrium was obtained and moduli increased. This was shown in precedent studies[27]

The experiment reported in Figure 3 correspond to a temperature sweeps. It was made without ageing, so as expected the moduli were lower than those obtained with ageing.

The results concerning runs 4 and 5 (Figure 3) show that the structure does not influence the temperatures of reversibility; for tri-armed and penta-armed structures, the same temperature of reversibility was obtained. However, a clear difference in the modulus values was noticed here. In fact, run 4 shows higher modulus values ($\sim 10^4$) than run 5 ($\sim 10^1$). This could be explained by the important steric effect that can be observed in the penta-armed structure.

Crossover temperatures representing the crosslinking/decrosslinking temperatures of the prepared networks are between 37 and 80 °C. These low temperatures allow the use of these materials in various applications in biomedical fields. However, 80 °C may be too low for several other applications; it is possible to increase the crossover temperature using additional dynamic reactions via Diels-alder reaction.[27] This will be examined in the next part.

Synthesis and Characterization of Hybrid Bioconjugated Networks

To prepare hybrid bioconjugated networks, glycerol and xylitol were used (run 6 and 7). The GSH arms number was fixed to two for both systems. A furan/maleimide Diels-Alder adduct was used to bring an additional dynamic covalent bonding to these systems. To analyse the effect of the dynamic interaction nature, networks prepared in runs 4 and 5 have been designed

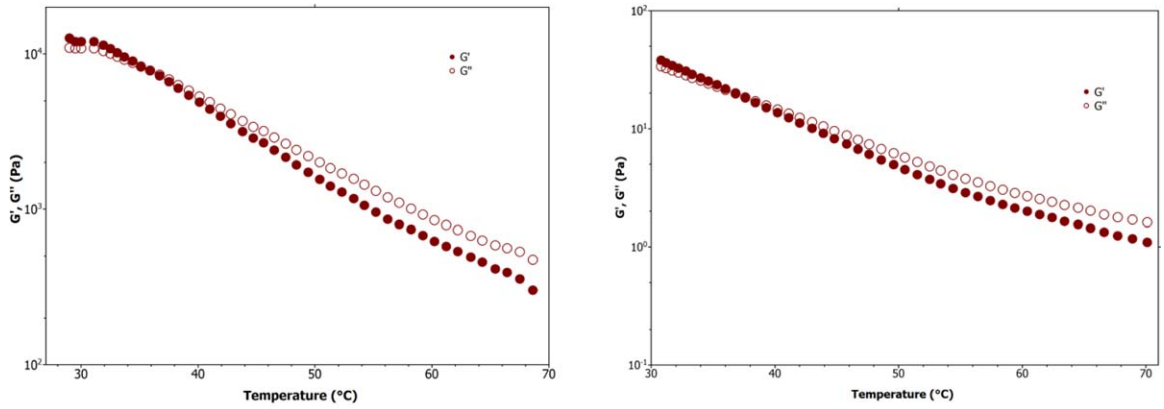

Figure 3. Dynamic temperature sweeps for the supramolecular bioconjugated systems (run 4 and 5) at 1 rad s^{-1} - first heating cycle. [Color figure can be viewed in the online issue, which is available at wileyonlinelibrary.com.]

with supramolecular interactions coming only form the gluthatione. Runs 6 and 7 had equivalent structures than 4 and 5, the difference is that a part of gluthatione was replaced by DA. From network 4 to 6, one part of gluthatione is replaced by one part of DA links. From network 5 to 7, three parts of gluthatione are replaced by three parts of DA links.

It should be noted that in runs 6 and 7 the dynamic part is kept voluntary identical but the DA fraction is higher in run 7 than in run 6.

A typical structure of a hybrid network was depicted in Scheme 3.

The thermal-dependence of these systems was evaluated by dynamic mechanical spectroscopy.

The networks showed a unique T_g measured by DSC and also only one sharp tan(δ) by dynamic mechanical spectroscopy. This demonstrated clearly that the obtained networks were homogeneous (1 phase).

Figure 4 shows results concerning hybrid double dynamic networks. The reversibility temperatures increased dramatically

Table II. Thermomechanical Properties of the Obtained Networks

Run	T_g (°C)	$T_{crossover}$ (°C)	G' (Pa)* E-5	M_c (kg mol^{-1})
Run 1	−25	50	6.54	3.95
Run 2	−14	80	20.30	1.27
Run 3	−13	76	3.00	8.60
Run 4	−29	36	4.21	6.13
Run 5	−47	37	0.00612	4217.12
Run 6	−27	112	37.50	0.69
Run 7	−32	86	0.361	71.49

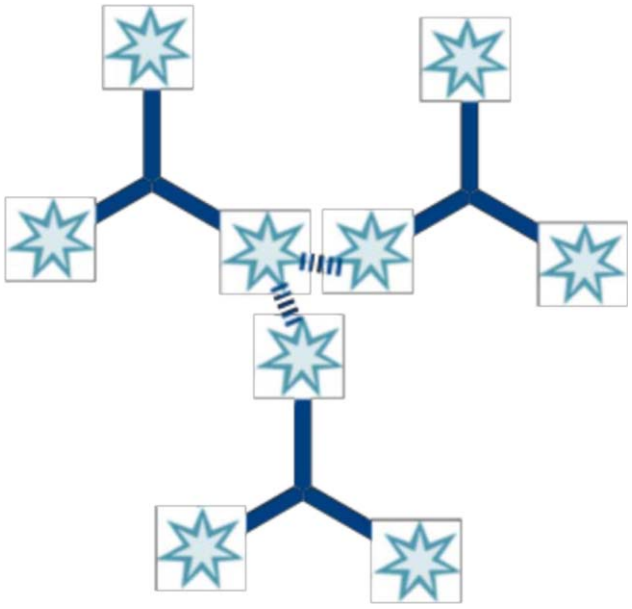

Scheme 2. Multiple hydrogen bonding in GSH molecules. [Color figure can be viewed in the online issue, which is available at wileyonlinelibrary.com.]

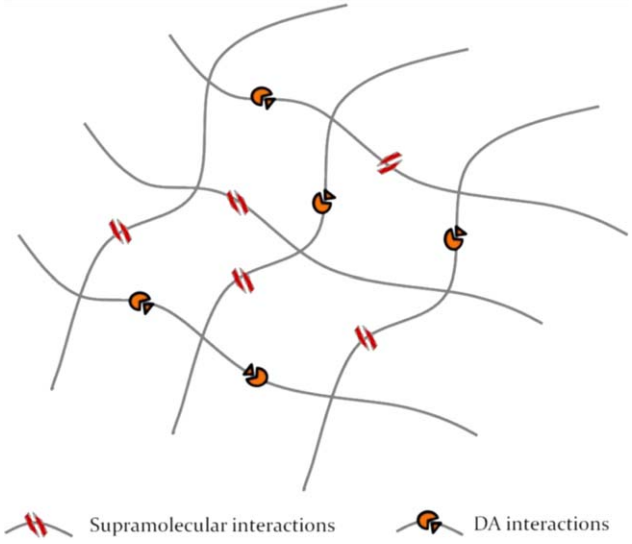

Scheme 3. Hybrid Network structure. [Color figure can be viewed in the online issue, which is available at wileyonlinelibrary.com.]

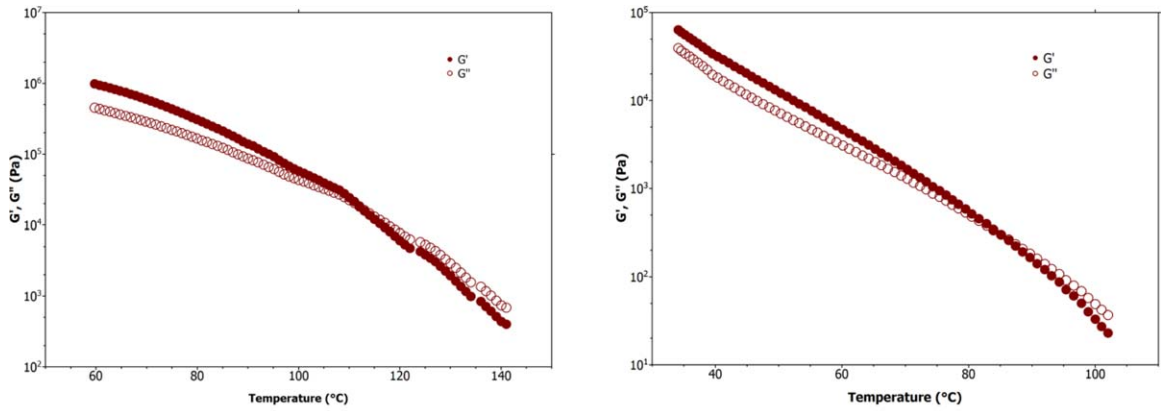

Figure 4. Dynamic temperature sweeps for the supramolecular bioconjugated systems (run 6 and 7) at 1 rad s^{-1} - first heating cycle. [Color figure can be viewed in the online issue, which is available at wileyonlinelibrary.com.]

compared with those measured for equivalent supramolecular networks. The same evolution was observed concerning the modulus values. In fact, storage modulus values increase by two decades in both systems compared to runs 4 and 5. In hybrid double dynamic networks, the steric effect of the penta-armed structure was confirmed, since it shows reversibility temperatures lower than the triarmed structure in spite of having 2 additional DA adduct moieties. An equivalent evolution was obtained in a previous study.[27]

The molar mass between crosslinks was also calculated for all the samples according to the following equation:

$$M_c = \left(\frac{G'}{\rho_{\text{Network}} RT}\right)^{-1} \quad (1)$$

where,

M_c is the molar mass between crosslinks.

R is the perfect gas constant.

G' is the storage modulus at the plateau at 1 rad s^{-1} at T: temperature.

ρ_{network} is the density of the network.

The thermomechanical properties of the obtained networks are quoted in Table II.

For linear systems (runs 1–3), M_c values show that for run 1 and 3 chain extension occurs. In fact, M_c values were 5 and 2.5 times bigger than the used PLA M_n for run 1 and 3, respectively. In contrast with that, the M_c value concerning run 2 was smaller than used PLA M_n, this could be explained by the presence of supplementary physical links.

DSC analysis shows that the glass transition temperature (T_g) of each of the studied networks was below room temperature. In

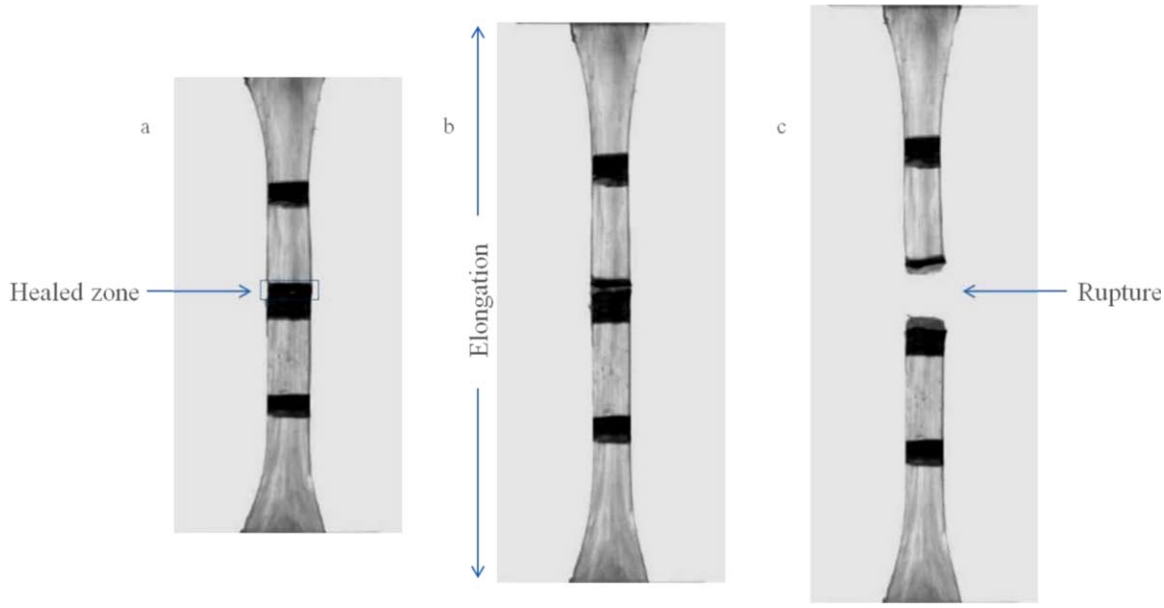

Figure 5. Self-healing tests for runs 2 and 6 at room temperature. [Color figure can be viewed in the online issue, which is available at wileyonlinelibrary.com.]

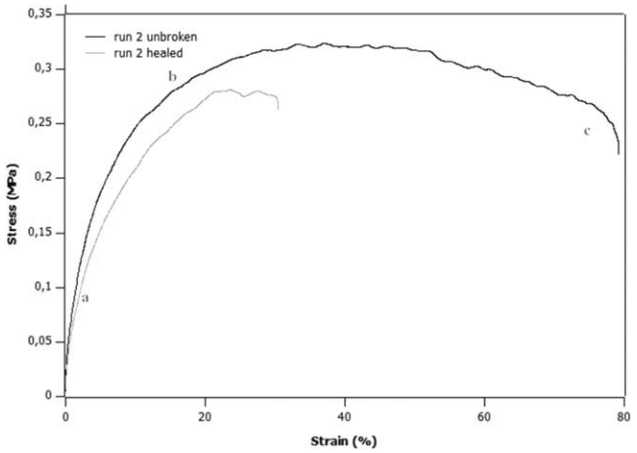

Figure 6. Stress-strain curves of run 2 - comparison between healed (dark line) and unbroken (gray line) samples.

linear systems (runs 1–3) T_g values tended to increase when the PLA molar masse from 800 to 2000 g Mol^{-1} than leveled.

For runs 4 and 5 compared with runs 6 and 7, T_g values increased when DA adducts were introduced (Table II), showing that the network was stronger with DA adducts. In addition, it can be noticed that Tcrossover value increases when DA adducts were added and denser networks were obtained (M_c decreased).

Self-Healing Tests

Self-healing tests were performed on two samples (runs 2 and 6). As shown in Figure 5, the samples were broken in the middle and then healed by manually reassembling the broken pieces together during typically 1 min. The reassembled samples were then left at room temperature for 24 h without application of any pressure.

The healing efficiencies of these materials were determined from tensile analyses (Figure 6). Comparison of the stress-strain curves of the healed samples corresponding to runs 2 and 6 and their original unbroken samples (Figure 5) demonstrate that the healed samples show practically the same tensile profile as the original unbroken samples. The healing efficiency was then evaluated as the ratio of the toughness of the repaired samples to that of the original sample.

Figure 6 Stress-strain curves of run 2—comparison between healed (dark line) and unbroken (gray line) samples.

Table III. Characteristics of Run 2 and 6 Healed and Unbroken Samples

Sample	Young's modulus (MPa)	Ultimate strength (MPa)	Elongation at break (%)
Run 2 unbroken	6.450	0.27	75
Run 2 healed	4.820	0.25	32
Run 6 unbroken	4.140	0.06	118
Run 6 healed	3.840	0.05	39

The healing efficiencies of runs 2 and 6 were of 43 and 33%, respectively, (Table III). These original results open up interesting outlooks for these new smart materials.

CONCLUSIONS

Using a peptide to synthesize bioconjugated materials allowed the formation of a reversible physical network thanks to hydrogen interactions between GSH molecules. On top of that, using this peptide in a Diels-Alder based network allowed the formation of an interesting and denser double dynamic system and offers the possibility to create novel conjugated PLA as self-healing materials. The healing efficiency of these materials was about 43% after just 24 h of repair at room temperature and without pressure.

ACKNOWLEDGMENTS

The authors are grateful to the Algerian Ministry of Higher Education and Scientific Research (MESRS) for the PhD scholarship fund of Dalila DJIDI.

REFERENCES

1. Duncan, R. *Nat. Rev. Drug Discov.* **2003**, *2*, 347.
2. Langer, R.; Tirrell, D. A. *Nature* **2004**, *428*, 487.
3. Veronese, F. M. *Biomaterials* **2001**, *22*, 405.
4. Zalipsky, S. *Adv. Drug Delivery Rev.* **1995**, *16*, 157.
5. Zhang, S. *Nat. Biotech.* **2003**, *21*, 1171.
6. Tu, R. S.; Tirrell, M. *Adv. Drug. Delivery Rev.* **2004**, *56*, 1537.
7. Whitesides, G. M. *Small* **2005**, *1*, 172.
8. Lutz, J.-F.; Börner, H. G. *Prog. Polym. Sci* **2008**, *33*, 1.
9. Börner, H. G. *Prog. Polym. Sci.* **2009**, *34*, 811.
10. Khandare, J.; Minko, T. *Prog. Polym. Sci.* **2006**, *31*, 359.
11. Pasut, G.; Veronese, F. M. *Prog. Polym. Sci.* **2007**, *32*, 933.
12. Van Hest, J. C. M. *J. Macromol. Sci. Part C: Polym. Rev.* **2007**, *47*, 63.
13. Larson, N.; Ghandehari, H. *Chem. Mater.* **2012**, *24*, 840.
14. Ponnumallayan, P.; Fee, C. J. *Langmuir* **2014**, *30*, 14250.
15. Bencherif, S. A.; Srinivasan, A.; Sheehan, J. A.; Walker, L. M.; Gayathri, C.; Gil, R.; Hollinger, J. O.; Matyjaszewski, K.; Washburn, N. R. *Acta Biomater.* **2009**, *5*, 1872.
16. Pelegri-O'Day, E. M.; Lin, E.-W.; Maynard, H. D. *J. Am. Chem. Soc.* **2014**, *136*, 14323.
17. Salmaso, S.; Bersani, S.; Mastrotto, F.; Tonon, G.; Schrepfer, R.; Genovese, S.; Caliceti, P. *J. Controlled Release* **2012**, *162*, 176.
18. Pasut, G.; Sergi, M.; Veronese, F. M. *Adv. Drug Delivery Rev.* **2008**, *60*, 69.
19. Veronese, F. M.; Harris, J. M. *Adv. Drug Delivery Rev.* **2002**, *54*, 453.
20. Alexis, F.; Basto, P.; Levy-Nissenbaum, E.; Radovic-Moreno, A. F.; Zhang, L.; Pridgen, E.; Wang, A. Z.; Marein, S. L.;

Westerhof, K.; Molnar, L. K.; Farokhzad, O. C. *Chem. Med. Chem.* **2008**, *3*, 1839.

21. Barwal, I.; Sood, A.; Sharma, M.; Singh, B.; Yadav, S. C. *Colloids Surf. B* **2013**, *101*, 510.
22. Li, Z. L.; Xiong, X. Y.; Li, Y. P.; Gong, Y. C.; Gui, X. X.; Ou-Yang, X.; Lin, H. S.; Zhu, L. J.; Xie, J. L. *J. Appl. Polym. Sci* **2010**, *115*, 1573.
23. Gauthier, M. A.; Klok, H.-A. *Chem. Commun.* **2008**, 2591.
24. Guadagno, L.; Raimondo, M.; Naddeo, C.; Longo, P. *Application of Self-Healing Materials in Aerospace Engineering*; Wiley-VCH Verlag GmbH & Co. KGaA: Weinheim, Germany, **2013**; Chapter *17*, p 401.
25. Kessler, M. R.; Sottos, N. R.; White, S. R. *Compos. A* **2003**, *34*, 743.
26. Djidi, D.; Mignard, N.; Taha, M. *Ind. Corp. Prod.* **2015**, *72*, 220.
27. Lehn, J. M. *Prog. Polym. Sci.* **2005**, *30*, 814.
28. Rowan, S. J.; Cantrill, S. J.; Cousins, G. R. L.; Sanders, J. K. M.; Stoddart, J. F. *Angew. Chem. Int.* **2002**, *41*, 898.
29. Imato, K.; Nishihara, M.; Kanehara, T.; Amamoto, Y.; Takahara, A.; Otsuka, H. *Angew. Chem. Int. Ed.* **2012**, *51*, 1138.
30. Chen, Y.; Kushner, A. M.; Williams, G. A.; Guan, Z. B. *Nat. Chem.* **2012**, *4*, 467.
31. Wang, Q.; Mynar, J. L.; Yoshida, M.; Lee, E.; Lee, M.; Okuro, K.; Kinbara, K.; Aida, T. *Nature* **2010**, *463*, 339.
32. Harada, A.; Kobayashi, R.; Takashima, Y.; Hashidzume, A.; Yamaguchi, H. *Nat. Chem.* **2011**, *3*, 34.
33. Capelot, M.; Montarnal, D.; Tournilhac, F.; Leibler, L. *J. Am. Chem. Soc.* **2012**, *134*, 7664.
34. Cordier, P.; Tournilhac, F.; Soulié -Ziakovic, C.; Leibler, L. *Nature* **2008**, *451*, 977.
35. Chen, X. G.; Dam, M. A.; Ono, K.; Mal, A.; Shen, H. B.; Nutt, S. R.; Sheran, K.; Wudl, F. *Science* **2002**, *295*, 1698.
36. Chen, X.; Wudl, F.; Mal, A. K.; Shen, H. B.; Nutt, S. R. *Macromolecules* **2003**, *36*, 1802.
37. Liu, Y. L.; Hsieh, C. Y. *J. Polym. Sci. Part A: Polym. Chem.* **2006**, *44*, 905.
38. Liu, Y. L.; Chen, Y. W. *Macromol. Chem. Phys.* **2007**, *208*, 224.
39. Zeng, C.; Seino, H.; Ren, J.; Hatanaka, K.; Yoshie, N. *Macromolecules* **2013**, *46*, 1794.
40. Kavitha, A. A.; Singha, N. K. *ACS Appl. Mater. Interfaces* **2009**, *1*, 1427.
41. Postiglione, G.; Turri, S.; Levi, M. *Prog. Org. Coat.* **2015**, *78*, 526.
42. Zhang, Y. C.; Broekhuis, A. A.; Picchioni, F. *Macromolecules* **2009**, *42*, 1906.
43. Yoshie, N.; Watanabe, M.; Araki, H.; Ishida, K. *Polym. Degrad. Stab.* **2010**, *95*, 826.
44. Zhang, J. J.; Niu, Y.; Huang, C. L.; Xiao, L. P.; Chen, Z. T.; Yang, K. K.; Wang, Y. Z. *Polym. Chem.* **2012**, *3*, 1390.
45. Plaisted, T. A.; Nemat-Nasser, S. *Acta Mater.* **2007**, *55*, 5684.
46. Peterson, A. M.; Jensen, R. E.; Palmese, G. R. *ACS Appl. Mater. Interfaces* **2010**, *2*, 1141.
47. Reutenauer, P.; Buhler, E.; Boul, P. J.; Candau, S. J.; Lehn, J. M. *Chem. Eur. J.* **2009**, *15*, 1893.
48. Yoshie, N.; Saito, S.; Oya, N. *Polymer* **2011**, *52*, 6074.
49. Bergman, S. D.; Wudl, F. *J. Mater. Chem.* **2008**, *18*, 41.
50. Palleau, E.; Reece, S.; Desai, S. C.; Smith, M. E.; Dickey, M. D. *Adv. Mater.* **2013**, *25*, 1589.
51. Ying, H.; Zhang, Y.; Cheng, J. *Nat. Commun.* **2014**, *5*, 3218.
52. Holten-Andersena, N.; Harringtonb, M. J.; Birkedalc, H.; Leed, B. P.; Messersmithd, P. B.; Leea, K. Y. C.; Waitee, J. H. *Proc. Natl. Acad. Sci. U.S.A.* **2011**, *108*, 2651.
53. Huang, L.; Yi, N.; Wu, Y.; Zhang, Y.; Zhang, Q.; Huang, Y.; Ma, Y.; Chen, Y. *Adv. Mater.* **2013**, *25*, 2224.
54. Phadkea, A.; Zhanga, C.; Armanb, B.; Hsuc, C. -C.; Mashelkard, R. A.; Leled, A. K.; Tauberc, M. J.; Aryab, G.; Varghesea, S. *Proc. Natl. Acad. Sci. U.S.A.* **2012**, *109*, 4383.
55. Fox, J.; Wie, J. J.; Greenland, B. W.; Burattini, S.; Hayes, W.; Colquhoun, H. M.; Mackay, M. E.; Rowan, S. J. *J. Am. Chem. Soc.* **2012**, *134*, 5362.
56. Tawney, P. O.; Synder, R. H.; Conger, R. P.; Leibbrand, K. A.; Stiteler, C. H.; Williams, A. R. *J. Org. Chem.* **1961**, *26*, 15.
57. Okhay, N.; Mignard, N.; Jegat, C.; Taha, M. *Des. Monomers Polym.* **2013**, *16*, 475.
58. Jegat, C.; Mignard, N. *Polym. Bull.* **2008**, *60*, 799.
59. Belkhir, K.; Shen, H.; Chen, J.; Jegat, C.; Taha, M. *Eur. Polym. J.* **2015**, *66*, 290.